Journal of Modern Optics
Publication details, including instructions for authors and subscription information:
http://www.tandfonline.com/loi/tmop20

Analysis of SNR for laser heterodyne detection with a weak local oscillator based on a MPPC

He-yong Zhang[ab], Shuai Zhao[a], Ting-feng Wang[a] & Jin Guo[a]
[a] Changchun Institute of Optics, Fine Mechanics and Physics, Chinese Academy of Sciences, State Key Laboratory of Laser Interaction with Matter, Changchun, 130033, China
[b] University of the Chinese Academy of Sciences, Beijing 10039, China
Published online: 13 Jan 2014.

To cite this article: He-yong Zhang, Shuai Zhao, Ting-feng Wang & Jin Guo (2013) Analysis of SNR for laser heterodyne detection with a weak local oscillator based on a MPPC, Journal of Modern Optics, 60:20, 1789-1799, DOI: 10.1080/09500340.2013.861525

To link to this article: http://dx.doi.org/10.1080/09500340.2013.861525

Journal of Modern Optics, 2013
Vol. 60, No. 20, 1789–1799, http://dx.doi.org/10.1080/09500340.2013.861525

Analysis of SNR for laser heterodyne detection with a weak local oscillator based on a MPPC

He-yong Zhang[a,b]*, Shuai Zhao[a], Ting-feng Wang[a] and Jin Guo[a]

[a]*Changchun Institute of Optics, Fine Mechanics and Physics, Chinese Academy of Sciences, State Key Laboratory of Laser Interaction with Matter, Changchun, 130033, China;* [b]*University of the Chinese Academy of Sciences, Beijing 10039, China*

(*Received 12 August 2013; accepted 29 October 2013*)

In order to avoid the influence of shot noise due to the powerful local oscillator (LO) in traditional heterodyne detection, the signal-to-noise ratio (SNR) was analyzed for laser heterodyne detection with a weak LO at the photon level. First, the expression for the SNR with a pulsed laser was applied to the condition of partial CW and weak LO laser heterodyne detection, the spectrum of the heterodyne signal with the center frequency 212 kHz was obtained, and the theoretical value of the SNR found to be in agreement with experiment. Second, the techniques of data segment fractionizing and power spectral sensity (PSD) averaging were used to investigate the SNR. The results show that the volume of the data required can be decreased by a factor of 10 compared with the traditional PSD averaging, the data resource is fully used while signal processing, and the signal-to-noise improved ratio (SNIR) nearly obeys the $\sqrt{m}$ rule (m is the averaging time) under a small quantity of data segments. Finally, the limiting factors about the SNIR during the PSD averaging have been determined so that good use can be made of the data.

Keywords: MPPC; weak local oscillator; PSD averaging

1. Introduction

In the last decade, many efforts have been devoted to the development and characterization of photon-number resolving detectors. Some studies on three-dimensional imaging laser radars with Geiger-mode (GM) avalanche photodiode arrays have been reported by Lincoln Laboratory, Massachusetts Institute of Technology [1–4]. Also, some experimental results for heterodyne detection with a weak local oscillator (LO) were obtained. Many efforts have been made to develop new multi-pixel photon counters (MPPCs). The MPPC is a solid state photo-detector, also known as the silicon photomultiplier. It is a photon-counting device consisting of multiple avalanche photodiode pixels connected in parallel and operating in GM. When photons enter a pixel while it operates in GM, the pulse output from the pixel is constant regardless of the number of photons. This means that each pixel provides only the information whether or not it received one or more photons. The output signal from the MPPC is proportional to the number of excited pixels. It is a relatively new and promising class of solid-state, low-level light sensor with potential in a multitude of applications such as high-energy physics, astronomy, bio-molecular imaging, and medical imaging [5–9]. At first glance, it may seem absurd to purposely use a weak LO for heterodyne detection. Most treatises on the subject assume an LO strength large enough to overcome the thermal and circuit noise, for that is how shot-noise-limited sensitivity is achieved [10–15]. But what if the receiver noise could be made to be close to zero? This can be obtained with a photon-counting detector, which has virtually no circuit noise, so very few LO photons are needed to approach shot-noise-limited performance. The very low noise of a photon-counting detector presents several benefits for heterodyne measurements, including low LO power requirements (especially important for detector arrays) and the ability to use the same detector for both coherent detection and direct detection. In this paper, we focused on the signal-to-noise ratio (SNR) analysis of the heterodyne detection with low LO using data segment fractionizing and power spectral sensity (PSD) averaging. The improvement of the SNR was obvious with the above method, and some limiting reasons have been discussed so we can establish some steady groundwork for the detection of weak signals with a low power laser heterodyne system.

2. Experimental setup

The experimental setup is shown in Figure 1. A light beam with a wavelength of 532 nm is transmitted from a single-frequency laser. The laser beam is incident on the surface of a rotating diffuser, which was driven by AC servo motor, and the rotating velocity of the diffuser can be adjusted through the changing of the driving voltage. The scattering photons from the diffuser were gathered by the telescope, and a set of attenuators were placed in front of the MPPC module. Of course, the LO beam is

*Corresponding author. Email: yonghezhang1116@126.com

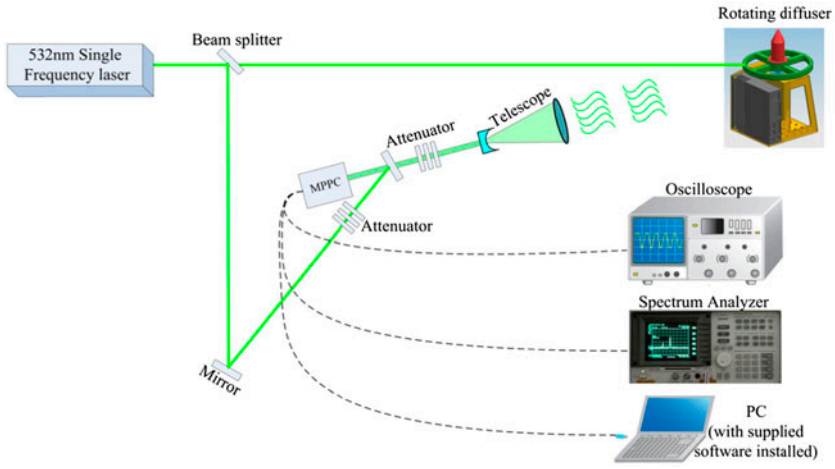

Figure 1. Sketch map of the photon counting heterodyne system with MPPC detectors (The colour version of this figure is included in the online version of the journal.)

also incident on the same MPPC detector surface with the same path while reflected by a beam splitter. The output from the MPPC module can be divided into three parts: the analog voltage output, comparator and the PC monitoring output.

Figure 1 shows that the analog voltage and the comparator outputs can be observed through an oscilloscope or a spectrum analyzer. The analog voltage output reflected the number of arriving photons and the arrival time. The amplitude of the voltage corresponded to the arriving photons during in the gated time (50 ns according to the MPPC detector), and 100 mV voltage denoted one arriving photon under theoretical conditions. In general, one arriving photon also called one photon event (pe) in the area of photon counting. The analog voltage and comparator outputs and the PC monitoring output are shown in Figure 2.

Figure 2(*a*) shows that the comparator output has about 20 ns time difference from the oscilloscope; this was determined by the inner circuit of the comparator. The threshold of the comparator can be modulated through the PC monitoring interface (Figure 2(*b*)).

3. The SNR of the weak LO heterodyne

There are many reports about the SNR and PSD analysis for photon counting heterodyne detection [3]. The main mathematical description will be given in this paper. This theory assumes that the initial phase of the beat signal is unknown and random from pulse to pulse. In other words, the coherent integration time is equal to the duration of the pulse but shorter than the pulse period. In general, this is a good assumption because both the movement of the target and the finite laser coherence time

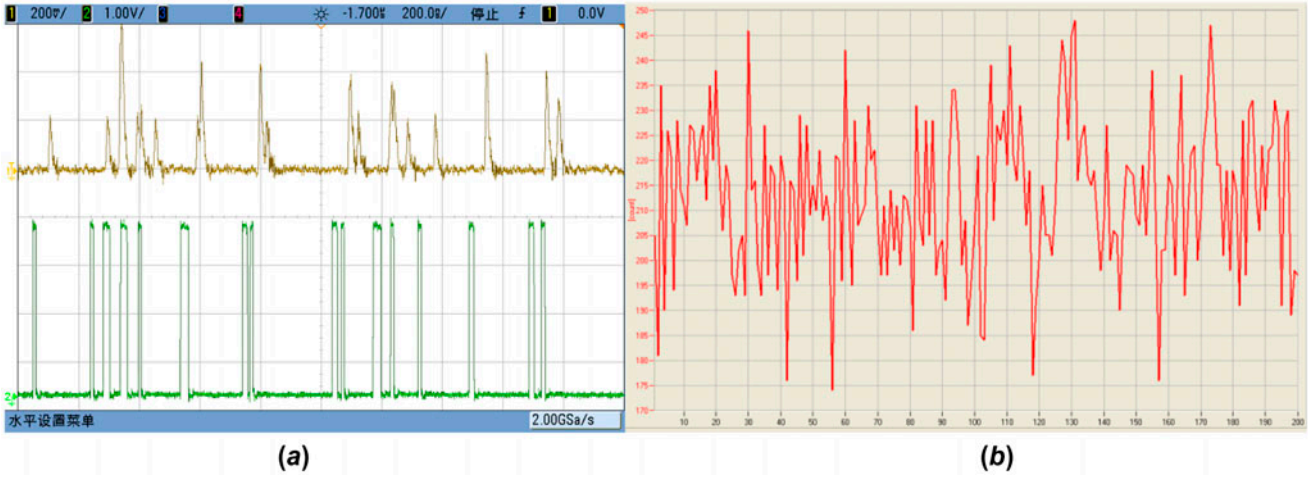

Figure 2. Waveform comparison between (*a*) the analog voltage and comparator outputs and (*b*) the PC monitoring output. (The colour version of this figure is included in the online version of the journal.)

will result in a random phase shift from pulse to pulse. If we consider the segmental continuous signal, the hypothesis above is approximately come into existence.

We start with the beat current between the laser echo and the LO. Taking the Fourier transform of this current yields the PSD per received pulse. Averaging several PSDs beats lowers the noise in the PSD and yields a strong peak at the intermediate frequency (f_{if}) of the target. The photon-counting detector that collects the incident signal and LO photons is a square-law detector and the resulting current is a sum of delta functions, where each delta function corresponds to a photoelectron event. The detected current for received pulse number k is equal to:

$$I^{(k)}(t) = \sum_{i=1}^{N_s^{(k)}+N_{LO}^{(k)}+N_D^{(k)}} \delta(t - t_i), \tag{1}$$

where N_S^k is the number of signal photoelectrons for the kth pulse, N_{LO}^k is the number of LO photoelectrons for the kth pulse, N_D^k is the number of dark counts for the same kth pulse, and t_i is the arrival time of the ith photoelectron. The bandwidth of the detector and electronics can be taken into account by replacing the delta function with the impulse response of the electronics. In any case, a threshold detector (such as the photon-counting detector) will record a discrete edge for the beginning of the pulse, so the impulse response of the electronics is largely irrelevant – although slow edges will result in larger timing jitter in the recording. In Fourier space, Equation (1) becomes the phasor sum:

$$\widetilde{I}^{(k)}(f) = \sum_{i=1}^{N_s^{(k)}+N_{LO}^{(K)}+N_D^{(k)}} \exp(-j2\pi f t_i) = \sum_{i=1}^{N_s^{(k)}+N_{LO}^{(K)}+N_D^{(k)}} \exp(-j\varphi_i), \tag{2}$$

where the phase φ_i is a product of the frequency f and the photon arrival times: $\varphi_i = 2\pi f t_i$, In the complex plane, for a given frequency, the sum of the phasors is analogous to the well-studied random walk problem, and the resulting two-dimensional (2-D) phase distribution function (PDF) for $\tilde{I}^{(k)}(f)$ is a 2-D Gaussian distribution. The distribution of the phasors for f_{n} is a 2-D Gaussian centered around the origin. The phasor sum for $f = f_{\mathrm{if}}$ is a 2-D Gaussian that has a nonzero mean (i.e. it is not centered at the origin). The reason for the nonzero mean is that the arrival times of the photons occur, on average, at intervals of $1/f_{\mathrm{if}}$.

For $f = f_{\mathrm{n}}$, the time intervals are completely random, so the phases of the individual phasors are independent of each other and uniformly distributed from $-\pi$ to π. For $f = f_{\mathrm{if}}$, the photon arrival times t_i are not random, but follow a sinusoidal PDF with a frequency that is equal to the beat frequency between the signal and LO. The resulting phases of the individual phasors then nearly line up and result in a nonzero mean for the 2-D Gaussian distribution. The distribution for the arrival times t_i can be derived from the classical expression for the current corresponding to a heterodyne signal for received pulse k:

$$I^{(k)}{}_{classical}(t) = N_S^{(k)} + N_{LO}^{(k)} + N_D^{(k)} + 2m\sqrt{N_S^{(k)}.N_{LO}^{(K)}}\cos(2\pi f_{if} t + \theta^{(k)}), \tag{3}$$

where m^2 is the mixing efficiency and $\theta^{(k)}$ is the initial phase. In Equation (3), we ignored the terms proportional to $\sqrt{N_S^{(k)}.N_D^{(k)}}\cos(2\pi f_{if} t)$ and $\sqrt{N_{LO}^{(k)}.N_D^{(k)}}\cos(2\pi f_{if} t)$ terms that are from the beating between the signal and the dark current spectral power at the LO frequency; and between the LO and the dark current spectral power at the signal frequency. These terms are much smaller than $\sqrt{N_S^{(k)}.N_{LO}^{(k)}}\cos(2\pi f_{if} t)$ and, hence, can be safely disregarded.

As implied by Equation (3), each received pulse has a different N_S and N_{LO} and a different initial phase. Since N_{LO} obeys a Poissonian distribution, the probability that there are q LO photoelectrons for pulse k is:

$$P_{N_{LO}^{(K)}}(q) = \frac{(\bar{N}_{LO})^q \exp(-\bar{N}_{LO})}{q!}, \tag{4}$$

where $\bar{N}_{LO}$ is the average number of LO photoelectrons per pulse averaged over all pulses and all time. In addition, we assume that the dark counts also obey a Poissonian distribution. The first and second moments of this distribution are given by

$$E[N_{LO}^{(k)}] = \bar{N}_{LO}, \tag{5}$$

$$E[(N_{LO}^{(k)})^2] = \bar{N}_{LO} + (\bar{N}_{LO})^2, \tag{6}$$

The number of signal photoelectrons, N_S, obeys a Poissonian distribution for a specular target and a negative binomial distribution for a diffuse target. For a diffuse target, the probability that there are q signal photoelectrons for pulse k is

$$P_{N_S^{(k)}}(q) = \frac{\Gamma(q+M)}{\Gamma(q+1)\Gamma(M)}\left(1+\frac{M}{\bar{N}_S}\right)^{-q}\left(1+\frac{\bar{N}_S}{M}\right)^{-M}, \tag{7}$$

where $\bar{N}_S$ is the average number of signal photoelectrons per pulse averaged over all speckle realizations and all pulses, and the parameter M represents the 'diffuseness' of the target or, more quantitatively, the number of degrees of freedom of the intensity included within the measurement interval. For example, detecting both polarizations doubles M. The smaller the value of M, the more diffuse the target. In the limit of large M, the negative binomial distribution converges to a Poissonian

distribution, i.e. the target can be treated as being effectively specular. The first and second moments of Equation (7) are given by

$$E\left[N_S^{(k)}\right] = \bar{N}_S, \tag{8}$$

$$E\left[(N_S^{(k)})^2\right] = \bar{N}_S + \left(1 + \frac{1}{M}\right)(\bar{N}_S)^2. \tag{9}$$

For a perfectly diffuse target with a polarizer before the detector so that only the vertical or the horizontal polarization of the scattered light is seen by the detector, $M = 1$, and the distribution given by Equation (7) simplifies to the Bose–Einstein (or geometric) distribution

$$P_{N_S^{(k)}}(q) = \frac{1}{1+\bar{N}_S}\left(\frac{\bar{N}_S}{1+\bar{N}_S}\right)^q. \tag{10}$$

The first and second moments of Equation (9) are given by:

$$E[N_S^{(k)}] = \bar{N}_S, \tag{11}$$

$$E\left[\left(N_S^{(k)}\right)^2\right] = \bar{N}_S + 2(\bar{N}_S)^2. \tag{12}$$

We now proceed to derive the PDFs for the magnitude of the single-pulse PSD at the signal and noise frequencies. Since the PSD averaged over k pulses is related to the detected current according to $PSD = (\frac{1}{K})\sum_{k=1}^{K}\left|\tilde{I}^{(k)}(f)\right|^2$, where $\tilde{I}^{(k)}(f)$ is given by Equation (2). Through the analysis of the amplitude and phase for $\tilde{I}^{(k)}(f)$, we can obtain the PSD of the intermediate frequency and the noise signal.

In this paper, the random variable G stands for the value of the PSD at a given frequency. Hereafter, for convenience we use G_{if} to denote the value of the PSD at $f = f_{\mathrm{if}}$ and G_n to denote the value of the PSD at $f = f_{\mathrm{n}}$. So the first and second moments of the intermediate frequency and the noise signal can be expressed:

$$E[G_{if}] = m^2\bar{N}_S\bar{N}_{LO} + (\bar{N}_S + \bar{N}_{LO} + \bar{N}_D), \tag{13}$$

$$\begin{aligned}E[G_{if}^2] = {} & 2(\bar{N}_S + \bar{N}_{LO} + \bar{N}_D) + 2(\bar{N}_S + \bar{N}_{LO} + \bar{N}_D)^2 \\ & + \frac{2\bar{N}_S^2}{M} + 4m^2\bar{N}_S\bar{N}_{LO}\bar{N}_D + m^4\left(1 + \frac{1}{M}\right)\bar{N}_S^2\bar{N}_{LO}^2 \\ & + m^2(m^2+8)\bar{N}_S\bar{N}_{LO} + m^2(m^2+4)\bar{N}_S\bar{N}_{LO}^2 \\ & + m^2(m^2+4)\left(1 + \frac{1}{M}\right)\bar{N}_S^2\bar{N}_{LO},\end{aligned} \tag{14}$$

$$E[G_n] = \bar{N}_S + \bar{N}_{LO} + \bar{N}_D, \tag{15}$$

$$E[G_n^2] = 2(\bar{N}_S + \bar{N}_{LO} + \bar{N}_D) + 2(\bar{N}_S + \bar{N}_{LO} + \bar{N}_D)^2 + \frac{2\bar{N}_S^2}{M}, \tag{16}$$

where m^2 is the mixing efficiency of the signal and LO photoelectrons. According to the expression of the variance:

$$\sigma_G^2 = E[G^2] - (E[G])^2, \tag{17}$$

the variance for a diffuse target can be evaluated as:

$$\begin{aligned}\sigma_{G_{if}}^2 = {} & 2(\bar{N}_S + \bar{N}_{LO} + \bar{N}_D) + (\bar{N}_S + \bar{N}_{LO} + \bar{N}_D)^2 \\ & + \frac{2\bar{N}_S^2}{M} + 2m^2\bar{N}_S\bar{N}_{LO}\bar{N}_D + \frac{m^4\bar{N}_S^2\bar{N}_{LO}^2}{M} \\ & + m^2(m^2+8)\bar{N}_S\bar{N}_{LO} + m^2(m^2+2)\bar{N}_S\bar{N}_{LO}^2 \\ & + m^2\left(m^2 + 2 + \frac{m^2+2}{M}\right)\bar{N}_S^2\bar{N}_{LO},\end{aligned} \tag{18}$$

$$\sigma_{G_n}^2 = 2(\bar{N}_S + \bar{N}_{LO} + \bar{N}_D) + (\bar{N}_S + \bar{N}_{LO} + \bar{N}_D)^2 + \frac{2\bar{N}_S^2}{M}. \tag{19}$$

According to the definition of the SNR:

$$SNR = \left(\frac{\bar{G}_{if} - \bar{G}_n}{\sigma_{G_{if}} + \sigma_{G_n}}\right)^2, \tag{20}$$

the SNR can be written as follows:

$$SNR = \frac{(m^2\bar{N}_S\bar{N}_{LO})^2}{\left(\begin{array}{l}\sqrt{\begin{array}{l}2(\bar{N}_S + \bar{N}_{LO} + \bar{N}_D) + (\bar{N}_S + \bar{N}_{LO} + \bar{N}_D)^2 + \frac{2\bar{N}_S^2}{M} \\ +2m^2\bar{N}_S\bar{N}_{LO}\bar{N}_D + \frac{m^4\bar{N}_S^2\bar{N}_{LO}^2}{M} + m^2(m^2+8)\bar{N}_S\bar{N}_{LO} \\ +m^2(m^2+2)\bar{N}_S\bar{N}_{LO}^2 + m^2(m^2+2+\frac{m^2+4}{M})\bar{N}_S^2\bar{N}_{LO}\end{array}} \\ +\sqrt{2(\bar{N}_S + \bar{N}_{LO} + \bar{N}_D) + (\bar{N}_S + \bar{N}_{LO} + \bar{N}_D)^2 + \frac{2\bar{N}_S^2}{M}}\end{array}\right)^2}.$$

The expression above shows that the SNR of the heterodyne signal can be estimated while giving the appropriate parameters. In this paper, the signal photoelectrons are equal to the LO photoelectrons; the experimental and theoretical results are shown in figure 3.

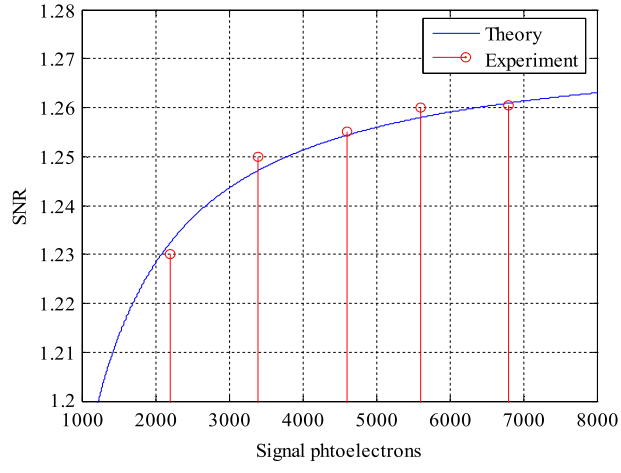

Figure 3. The SNR of the photon counting heterodyne system. (The colour version of this figure is included in the online version of the journal.)

The abscissa in Figure 3 indicates the number of the integral signal photoelectrons output from the MPPC detector in one millisecond. In the course of the simulation, the mixing efficiency m^2 is 0.2, parameter M is 1.275 (M = 1 corresponds to the ideal diffuser, the target in the experiment was covered with white paper), the dark count rate is 0.9 kcps (kilo counts per second). The graph in Figure 3 shows that the experimental and theoretical results are consistent with each other during the selection of proper input parameter. So we can see the SNR expression of the weak LO heterodyne in pulsed laser seems reasonable during the analysis of the SNR for segmental continuous heterodyne detection.

4. PSD of the photon counting heterodyne

The Doppler frequency shift can be achieved from the analysis of the PSD for the photon counting heterodyne signal, but the noise of the echo signal will affect the frequency distinguishing due to the reflecting surface and the atmospheric transmission paths. Therefore, some de-noising methods should be adopted to improve the SNR of the beat signal. But the noise mentioned in this paper is in frequency domain, so time domain or space domain methods such as matched filtering, bandpass filtering, or autocorrelation have no excellent function. Consequently, we must find some reasonable and effective techniques to overcome the decline of the SNR. Fortunately, the method of PSD averaging has been used diffusely in the frequency domain for many decades, and this method also proved to be applicable in the area of photon counting heterodyne (weak LO) detection by some researchers under the condition of pulsed laser. We mainly focus on the implication of this method while the incident laser is segmental continuous (such as the continuous laser pass through the chopper).

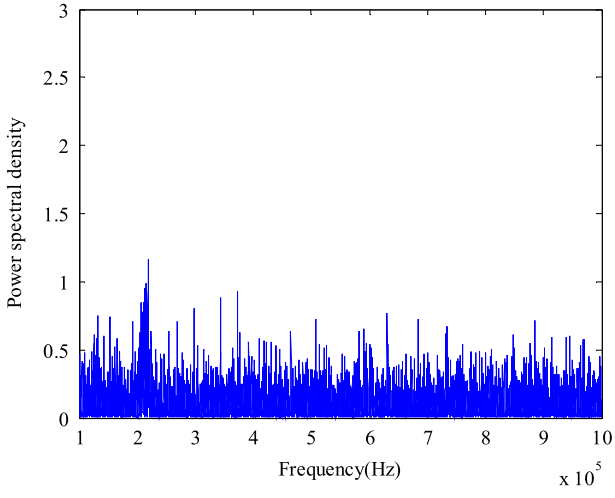

Figure 4. The power spectrum of the heterodyne signal with single measurement. (The colour version of this figure is included in the online version of the journal.)

4.1. The traditional PSD averaging

The length of the experimental data is 4,000,000, the sampling rate is 400 MHz, and the total time for all of the data is 10 ms. The single PSD of some original experimental data is shown in Figure 4.

Figure 4 shows that the peak value of the PSD is located at 212 kHz, but that it has low SNR. In order to improve the SNR of the beat signal, the traditional PSD averaging method was applied while using 5, 10, 15, or 20 data segments (Figure 5).

As shown in Figure 5, the SNR has enhanced by 3–4 times while introducing the PSD averaging for 20 data segments (with data length = 4,000,000). But the background noise is still strong; therefore, a method named data segment fractionizing and PSD averaging has been put forward to improve the SNR of the beat signal. The core of the technique is truncating the raw data for several small segments, then, giving the PSD sum of the all data segment, the SNR will increase with this operation.

4.2. Data segment fractionizing and PSD averaging

As explained before, we have improved the SNR by averaging the 20 PSDs through the traditional PSD averaging method to some extent, and the data length is 4,000,000 (the depth of the FFT is 2^{22} = 4,194,304), but has no obvious effects. So the data segment fractionizing and PSD averaging method has been adopted in order to achieve large-scale SNR improvement. We have mentioned the fractionizing of the original data, but how to decide the length of the smaller data segment is important in the processing, because the SNR of the fractionized data segments has some restriction, as explained in the following.

4.2.1. The times of PSD averaging

The method of PSD averaging has effects in improving the SNR due to the statistical property of the noise and the signal; the PSD of the noise is disordered versus the frequency, but the signal's PSD will keep some peak value at a fixed frequency point. From this single theory, we had hoped that the times of the PSD averaging would increase, so the SNR would achieve stable enhancement, but the experiment results did not accord with our theoretical prediction.

4.2.2. The duration of the data segment

The larger the time of PSD averaging, the shorter duration of each data segment for the fixed original data.

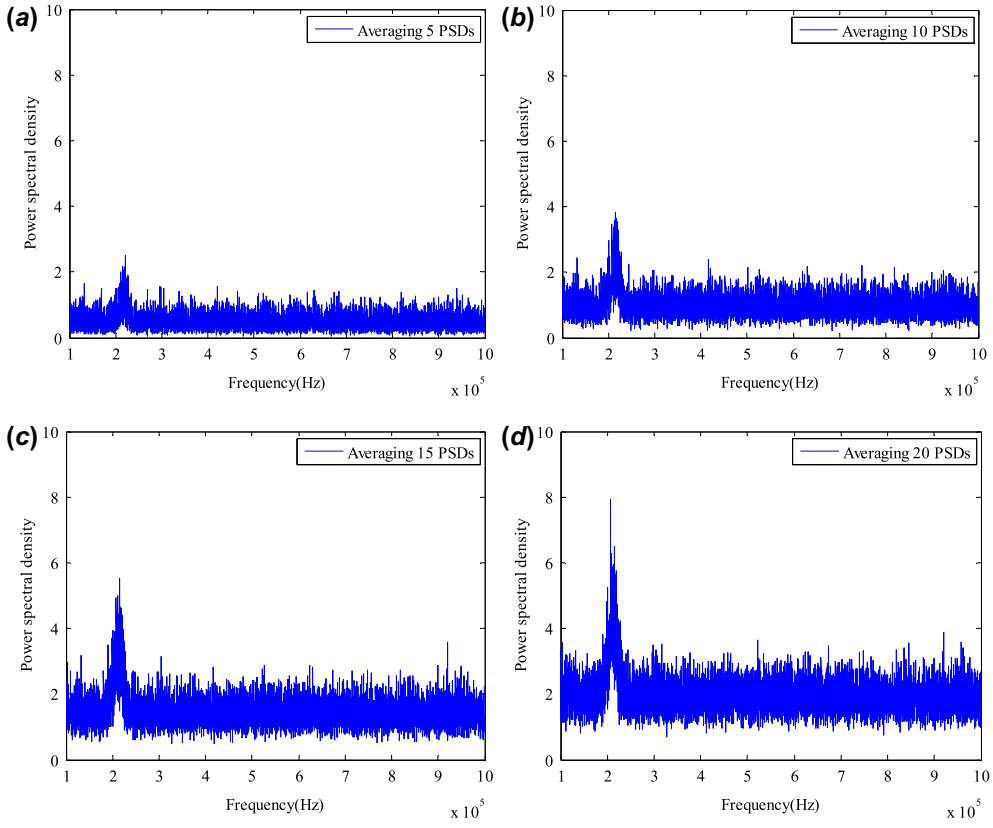

Figure 5. The averaged power spectrum of the heterodyne signal with several measurements. PSD accumulating with (*a*) 5, (*b*) 10, (*c*) 15, and (*d*) 20 data segments. (The colour version of this figure is included in the online version of the journal.)

This means that the number of signal periods decrease, or, in other words, the echo photons become weak. Therefore, the peak value of PSD for the signal will decrease due to the reduction of the data segment's duration according to the FFT theory, so the anti-noise ability will be weakened. From this single theory, we hope that the longer the data length (or duration) the better, which means that the times of PSD averaging will be reduced for the fixed-length original data. This phenomenon conflicts with the restriction condition explained above.

In order to obtain the comparison of the data segments before and after the fractionizing, we first give the PSD averaging after the one tenth division. Therefore, the original PSD averaging for 5, 10, 15, and 20 data segments become 50, 100, 150, and 200 short data segments PSD averaging. At this time, the data length in time domain was condensed into one tenth of the original data length, but the points of the FFT have no change before and after the data length condensing so that the frequency resolution remains unchanged. At the same time, we give the PSD averaging of the first 10 and 20 short data segments in order to show the improvement of the SNR. So, the six PSD averaging situations are shown in Figure 6(*a*) to 6(*f*), respectively.

From Figure 6, it can be seen that the first 20 PSD averaging of the short data segments has a similar SNR to the original 20 PSD averaging of the long data segments (equal to 200 short data segments after fractionizing). In other words, the data size has only about 1/10 of the original data length after data fractionizing, while it has the same SNR. This is important in real-time data processing and effective use of memory cells. We can draw the following conclusions from the six results in Figure 6.

Firstly, the SNR increases with an increase of the number of PSD averaging steps, as shown in Figures 6(*a*)–6(*c*).

Secondly, the SNR has no obvious increase on further raising the number of PSD averaging steps (Figures 6(*d*)–6(*f*)). In other words, the improvement of the SNR appears to exhibit saturation effects.

Thirdly, the PSD in the low frequency range (near the DC component) has an obvious increase in each result in Figure 6 compared with those in Figure 5. This is harmful for signal extraction in the low frequency area.

Now, we will give some detailed analysis about these three conclusions.

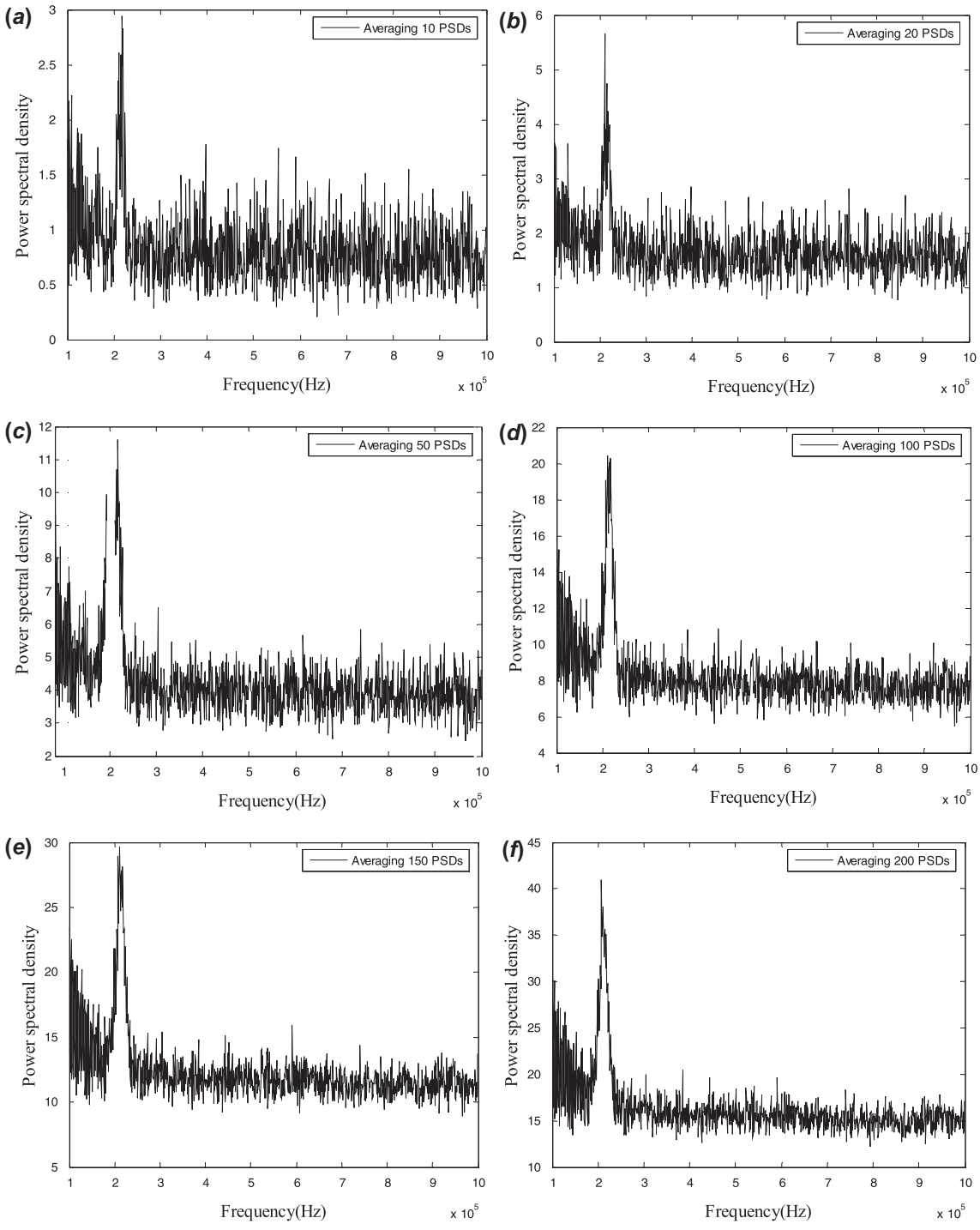

Figure 6. The averaged power spectrum of the heterodyne signal with several measurements after data fractionizing. PSD accumulating with the first (*a*) 10, (*b*) 20, (*c*) 50, (*d*) 100, (*e*) 150, and (*f*) 200 short segments.

5. SNR enhancement for data segment fractionizing

5.1. The principle of SNR enhancement for data segment fractionizing

Most of the time, the consideration is always of improving SNR in either time domain or space domain, and the noise is usually supposed to be white Gaussian noise. This kind of noise has the property of a constant power spectrum, but a practical signal does not have this property. The power spectrum always fluctuates around a certain value during all time; this is similar to a

stationary random process. Therefore, the method of SNR enhancement in the frequency domain can draw lessons from signal averaging in time domain. For the sake of convenience, the whole course was considered as linear averaging, and the useful signal and noise can be written as:

$$f(t) = f_s(t) + n(t), \tag{22}$$

where $f_s(t)$ is the periodic signal and $n(t)$ is noise. If we sample the periodic signal at a fixed point with time interval T at the starting time t_k, then the ith sampling can be expressed as:

$$f(t_k + iT) = f_s(t_k + iT) + n(t_k + iT), \tag{23}$$

where i is the sampling ordinal number. For a periodic signal and synchronous sampling, the starting time t_k can be supposed as zero, so the expression above becomes:

$$f_s(t_k + iT) = f(iT). \tag{24}$$

The summation of the ith sample after m repeated samplings is:

$$\sum_{i=1}^{m} f(t_k + iT) = \sum_{i=1}^{m} f_s(iT) + \sum_{i=1}^{m} n(t_k + iT). \tag{25}$$

The signal after m summations can be written as:

$$\sum_{i=1}^{m} f_s(iT) = m f_s(iT), \tag{26}$$

But the noise after m summations will increase with the rules of statistical average enhancement:

$$\sum_{i=1}^{m} n(t_k + iT) = \sqrt{n_1^2(t_k + T) + n_2^2(t_k + 2T) + \ldots + n_m^2(t_k + mT)}, \tag{27}$$

If the averaging effective value for each noise sampling is $\overline{n(t)}$, then the noise after m samplings is:

$$\sum_{i=1}^{m} n(t_k + iT) = \sqrt{m[n(t)]^2} = \sqrt{m} \cdot \overline{n(t)}. \tag{28}$$

Therefore, the SNR after m times averaging is:

$$SNR|_m = \left(\frac{S}{N}\right)_m = \frac{m f_s(iT)}{\sqrt{m} \cdot \overline{n(t)}} = \sqrt{m} \frac{f_s(iT)}{n(t)} = \sqrt{m} \cdot \left(\frac{S}{N}\right)_{in}, \tag{29}$$

and the signal-to-noise improved ratio (SNIR) is:

$$SNIR|_m = \left(\frac{S}{N}\right)_m = \frac{SNR_m|_{out}}{SNR_m|_{in}} = \frac{\sqrt{m} \cdot (S/N)_{in}}{(S/N)_{in}} = \sqrt{m}. \tag{30}$$

We can see from the expression above that the SNIR obeys the $\sqrt{m}$ law after m times sampling averaging. In other words, the SNR will increase with many samples averaging for a periodic or repeating signal, and the more the averaging times, the higher the SNR. This method mentioned the periodic signal; in fact, the peak signal in frequency domain is similar to periodic signal, and the more the data segments, the more the signal period. Therefore, the SNR in frequency domain will be enhanced due to the data segment fractionizing method. The theoretical and experimental results are shown in Figures 7(a) and 7(b) for different experiments.

The improvement of SNR was consistent with theoretical forecast after 10 times of averaging, as shown in Figure 7. This shows that the averaging method in time domain can be used in frequency domain, but the premise is that the noise remains highly random, and this property cannot be described with a single Gaussian white noise process. On the contrary, the total noise contains various kinds of noise; therefore, the averaging method in frequency domain certainly will have much difference with the same method in time domain.

5.2. *The reason why the SNIR has no obvious increase*

The statement above has illustrated that the signal averaging in time domain and frequency domain have much difference, at last, the theory and experiment has much divergence due to the averaging times increasing. The SNIR of the first 50 short data segment averaging steps are shown in Figures 8(*a*) and 8(*b*) for different experiments.

As can be seen from Figure 8, the theory and experiment exhibit good consistency under a fewer averaging times (such as 10 times), but the offset between theory and experiment becomes much greater when the averaging times increases, with the experimental value always lower than the theoretical calculation. The reasons for this are as follows.

First, the statistical property of the noise in frequency domain is not a stationary random process. Therefore, the averaging results cannot obey the regulation of statistics enhancement, and this reason results in the statistical average value increasing, with the SNR decreasing.

Second, the periodicity of the frequency signal has been destroyed because of the outside interference and the stabilization of the processing system. This reason will cause the averaging signal amplitude less than m times of the initial amplitude, so the SNR will decrease compared with the theory.

It can be seen from the two reasons above that the segment fractionizing and PSD averaging has the ability for SNR enhancement, but the increment speed gradually reduces while increasing the averaging times. Consequently, we must select appropriate averaging

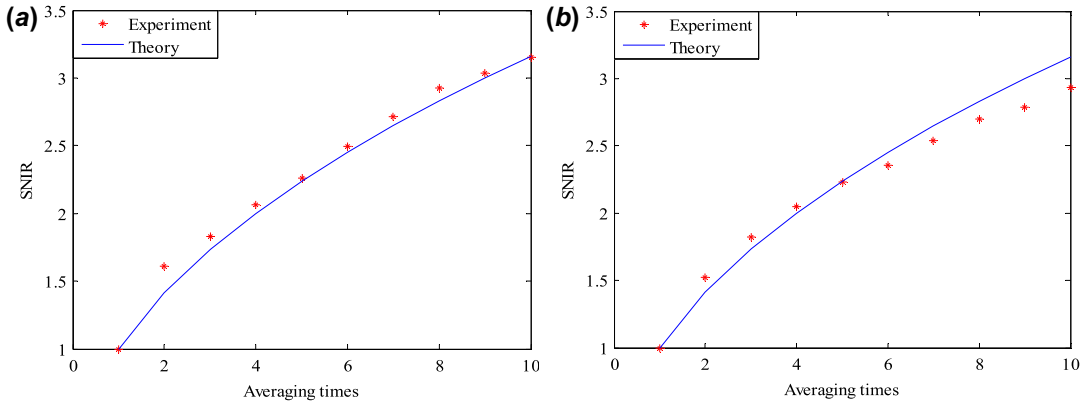

Figure 7. The SNR enhancement of the first 10 short data segments of the heterodyne signal after data fractionizing. The (*a*) first and (*b*) second experimental results. (The colour version of this figure is included in the online version of the journal.)

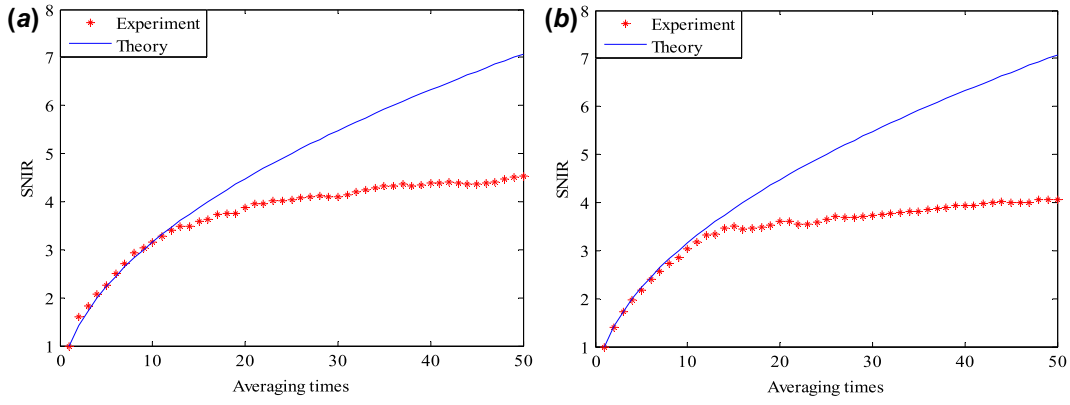

Figure 8. The SNR enhancement of the first 50 short data segments of the heterodyne signal after data fractionizing. The (*a*) first and (*b*) second experimental results. (The colour version of this figure is included in the online version of the journal.)

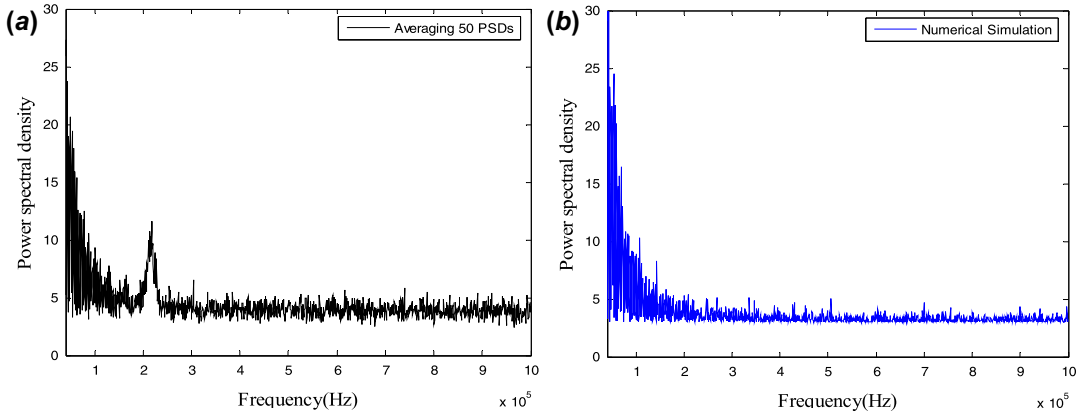

Figure 9. The (*a*) experimental and (*b*) numerically simulated results for the influence of the DC component. (The colour version of this figure is included in the online version of the journal.)

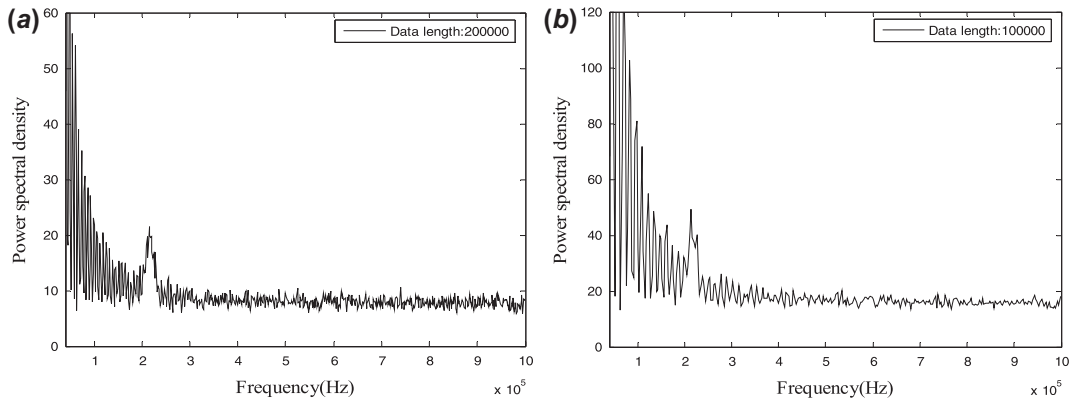

Figure 10. The influence of the DC component under different data lengths: (*a*) 200,000; (*b*) 100,000.

times for effective SNR increases, and it is not necessary to seek redundant short data segments averaging.

5.3. *The influence of DC signal component*

The analysis above showed that PSD averaging can improve the SNR, and the method of PSD averaging based on data segment fractionizing shows significant improvement compared with the original PSD averaging. However, the influence of DC component becomes more serious while the data length shorter. The numerical simulation of the influence of DC signal (has no useful signal peak) and the experiment result are shown in Figure 9.

The total length of the simulation is 4,000,000 points, the corresponding time span is 10 ms (which is divided equally into 10 small segments), and the sample rate is 400 MHz. From the expression of finite time constant amplitude oscillation:

$$E(t) = \begin{cases} A \cdot \exp(-i2\pi v_0 t) \rightarrow -T/2 \leqslant t \leqslant T/2 \\ 0 \rightarrow \text{The others} \end{cases}, \quad (31)$$

the corresponding PSD is:

$$|E(v)|^2 = T^2\{\sin c[T(v - v_0)]\}^2. \quad (32)$$

Now the definition of the spectrum width can be given as the two-frequency space for the PSD decline as the half of the peak value. Then, the spectrum width is $\Delta v = 1/T$, and the parameter T is the signal period (the time span for non-periodic signal). Therefore, the shorter the data length, the wider the spectrum width from the analysis above. This is the reason that the DC component has more influence while the data length becomes shorter. If the useful signal is near the DC component, signal extraction will be difficult. The results of an experiment showing the influence of DC component with different data length are provided in Figure 10.

As can be seen from Figure 10, the shorter the data length, the more severe the impact of DC component. So the choice of data length during the course of data segment fractionizing and PSD averaging should depend on the signal frequency.

6. Conclusion

In this paper, we have applied the SNR expression of a weak LO pulsed laser heterodyne signal to the analysis of partial CW laser heterodyne detection based on the MPPC module. The theoretical simulations and experimental results exhibit good agreement during the research, and the center frequency of the useful signal is 221 kHz. According to the definition of SNR, we have given the comparison of the SNR of the traditional PSD averaging and the PSD averaging after data segment fractionizing. The experimental results showed that when the data volume is reduced by a factor of 10 compared with the original data under the same SNR value, the availability of the measured data has improved greatly. Moreover, the SNIR after data segment fractionizing and PSD averaging obeys the $\sqrt{m}$ law after m times sampling averaging, but the SNIR will appear saturated due to the increase of averaging data volume. Meanwhile, we must pay attention to the influence of DC component in the course of data segment fractionizing and PSD averaging, especially for the low-frequency signal processing.

References

[1] Aull, B.F.; Loomis, A.H.; Young, D.J.; Heinrichs, R.M.; Felton, B.J.; Daniels, P.J.; Landers, D.J. *Lincoln Lab. J.* **2002,** *13*, 335–350.
[2] Albota, M.A.; Aull, B.F.; Fouche, D.G.; Heinrichs, R.M.; Kocher, D.G.; Marino, R.M.; Mooney, J.G.; Newbury, N.R.; O'Brien, M.E.; Player, B.E.; Willard, B.C.; Zayhowski, J.J. *Lincoln Lab. J.* **2002,** *13*, 351–370.
[3] Jiang, L.A.; Luu, J.X. *Appl. Opt.* **2008,** *47*, 1486–1503.

[4] Luu, J.X.; Jiang, L.A. *Appl. Opt.* **2006,** *45*, 3798–3804.
[5] Kim, C.L.; Wang, G.-C.; Dolinsky, S. *IEEE Trans. Nucl. Sci.* **2009,** *56*, 2580–2585.
[6] Minamino, A.; Nagai, N.; Orme, D.; Nakaya, T.; Yokoyama, M.; Nakadaira, T.; Murakami, T.; Tanaka, M.; Retiere, F.; Vacheret, A.; Kudenko, Y. *IEEE Nucl. Sci. Symp. Conf. Rec.* **2008,** *50*, 3111–3114.
[7] Gottlich, M.; Garutti, E.; Kozlov, V.; Schultz-Coulon, H.-C.; Tadday, A.; Terkulov, A. *IEEE Nucl. Sci. Symp. Conf. Rec.* **2008,** *50*, 3119–3122.
[8] Retiere, F.; Du, Y.; Foreman, S.; Kitching, P.; Kostin, A.; Lindner, T.; Low, M.; Masliah, P.; Moult, I.; Oser, S.; Tanaka, H.; Vacheret, A. *Nucl. Instrum. Methods Phys. Res., Sect. A* **2009,** *610*, 378–380.
[9] Henseler, D.; Grazioso, R.; Zhang, N.; Schmand, M. *IEEE Nucl. Sci. Symp. Conf. Rec.* **2009,** *28*, 1941–1947.
[10] Jakeman, E.; Oliver, C.J.; Pike, E.R. *Adv. Phys.* **1975,** *24*, 349–405.
[11] Liu, L.-S.; Zhang, H.; Guo, J.; Liu, H.; Zhao, S. *Opt. Precis. Eng.* **2011,** *19*, 2366–2372.
[12] Zhang, H.; Zhao, S.; Guo, J.; Wang, T.; Liu, H. *Opt. Precis. Eng.* **2012,** *20*, 2132–2139.
[13] Zhao, S.; Guo, J.; Liu, H.; Feng, Q. *Opt. Precis. Eng.* **2011,** *19*, 972–976.
[14] Liu, L.; Zhang, H.; Zhao, S.; Guo, J. *Acta Opt. Sin.* **2012,** *32*, 403001.
[15] Zhang, H.; Guo, J.; Zhao, S.; Wang, T.; Liu, L. *Chin. J. Lasers* **2011,** *38*, 100801.